Computational Fluid Dynamics and Data–Based Mechanistic Modelling of a Forced Ventilation Chamber ⋆

O. Tate * **E. D. Wilson** * **D. Cheneler** * **C. J. Taylor** *

* *Engineering Department, Lancaster University, UK*
(e-mail: o.tate@lancaster.ac.uk, e.d.wilson1@lancaster.ac.uk, d.cheneler@lancaster.ac.uk, c.taylor@lancaster.ac.uk)

Abstract: The research behind this article ultimately concerns control system robustness and optimisation for the regulation of temperatures in multiple buildings that are linked to a controllable external heating supply network. Lancaster University campus is being used as a case study, for which the building management system provides data. Nonetheless, situations arise when it is difficult or expensive to obtain suitable data for specific rooms or buildings and, in such cases, computational fluid dynamics (CFD) models are utilised to investigate relevant heat transfer phenomena. Such models can be limited by their complexity and they are inappropriate for model–based control design. Hence, the present article investigates a hybrid approach based on both CFD and data–based mechanistic (DBM) models. DBM models are obtained initially from statistical analysis of observational time–series but are only considered credible if they can be interpreted in physically meaningful terms. A laboratory forced ventilation chamber is used to investigate the modelling issues arising and to make recommendations relating to the wider project. The chamber is first discretised into finite volumes and the associated Navier–Stokes equations are solved to determine the physical properties of each zone. The model responses are compared with experimental data and analysed using the DBM approach.

Keywords: Computational fluid dynamics (CFD); data–based mechanistic (DBM); heating, ventilation and air conditioning (HVAC); micro–climate.

1. INTRODUCTION

The research behind this article concerns control system robustness and overall system optimisation, for the regulation of temperatures in buildings that are linked to a controllable external heating supply network. This is the case, for example, with the Lancaster University campus, for which a central energy centre supplies the hot water used to heat around 50% of the buildings (Ioannou, 2016). The authors are developing demand–side control concepts (e.g. Kim, 2013) to address multiple buildings on this network, i.e. the control actions for one building are accounted for when choosing actions for the other buildings, potentially increasing energy efficiency and improving thermal conditions for the building occupants.

Heating, Ventilation and Air Conditioning (HVAC) systems have high energy requirements, hence there is considerable interest in the development of improved optimisation tools, micro–climate control algorithms and energy management systems. Although the literature is vast, selective examples of such research include Yang and Wang (2013), Kim (2013), Goyal et al. (2013), Kossak and Stadler (2015) and Mayer et al. (2017), while Mirinejad et al. (2012) and Lazos et al. (2014) provide useful reviews focusing on intelligent control and energy management, respectively.

Numerous approaches for modelling heat transfer phenomena and energy use have been developed over the past few decades. The models obtained are commonly categorised into either physically–based models or models that are statistically identified from data (Foucquier et al., 2013). Whilst the former include various zonal and multi–zone approaches, CFD models are probably the most widely used in practice. CFD models consist of deterministic equations based on the classical laws of physics (e.g. Hong et al., 2017). However, such models are limited by their complexity and they are generally inappropriate for model–based control design.

Data–based models, by contrast, are usually much simpler and are identified using techniques from the machine learning or system identification literature. Examples in the context of building micro–climate include the consideration of well–mixed zones (Janssens et al., 2004), genetic algorithms (Ryozo and Kazuhiko, 2009), change point models (Paulus et al., 2015) and Hammerstein model forms (Tsitsimpelis and Taylor, 2014), among many others. Various hybrid approaches have also been proposed. For example, Agbi et al. (2012) apply data–based methods to multi–zone thermal systems, while Price et al. (1999) develop data–based mechanistic (DBM) models for agricultural buildings. DBM models are obtained initially

⋆ This work is supported by Engineering and Physical Sciences Research Council (EPSRC): EP/M015637/1. The DBM modelling algorithms are available within the CAPTAIN toolbox, which may be downloaded from: http://www.lancaster.ac.uk/staff/taylorcj/tdc.

from the analysis of observational time–series but are only considered credible if they can be interpreted in physically meaningful terms (Young, 2011). It is a philosophy that emphasises the importance of parametrically efficient, low order, dominant mode models, as well as the development of stochastic methods and the associated statistical analysis required for their identification and estimation (Young, 2011; Taylor et al., 2018). Finally, several authors have utilised a combined CFD and DBM modelling approach (Desta et al., 2004a,b; Steeman et al., 2009), a concept that is taken up in the present work.

Lancaster University's main campus is well suited for research into the optimisation of energy efficiency because of the existing data collection capacity from the building management system. Nonetheless, situations arise where it is difficult or expensive to obtain suitable data for specific rooms or buildings and, in such cases, CFD models are being utilised to investigate relevant heat transfer phenomena, and to optimise the placement of new sensors. Hence, following a similar approach to Desta et al. (2004b), the present article considers both CFD and DBM methods. In this mainly discursive, preliminary article, these are initially investigated using a laboratory forced ventilation test chamber (Tsitsimpelis and Taylor, 2014, 2015). The CFD and DBM methods utilised for this research are briefly reviewed in section 2, followed by their application to the ventilation chamber in sections 3 and 4. Finally, the discussion in section 5 has suggestions for how these results will be extended to the wider context of the campus energy management project.

2. METHODOLOGY

The two modelling approaches and laboratory rig are briefly introduced.

2.1 CFD Modelling

The airspace is discretised into finite volumes and the Navier–Stokes equations for the conservation of mass, momentum and total energy are solved, in order to determine the physical properties of each zone. The present work uses the Fluent component of the well–known ANSYS package (Fluent 17.2, 2016, ANSYS Inc). ANSYS is an amalgam of several programs that are widely used in both industry and academia. The basic steps in the modelling process are: define the geometry; discretise into small regions (called meshing); define the physical properties and boundary conditions; set the type of simulation; and, finally, solve and extract the desired information from the solution.

2.2 DBM Modelling

Transfer Function (TF) models are identified from experimental or CFD data using the Simplified Refined–Instrumental Variable (SRIV) algorithm (e.g. Young, 2011; Taylor et al., 2013, Chapter 8), implemented within the CAPTAIN Toolbox for Matlab (Taylor et al., 2007, 2018). Although not the focus of the present article, one novelty of the DBM approach for micro–climate modelling is the use of Agglomerative Hierarchical Clustering (AHC) to quantitatively distinguish and group thermal zones within the airspace for any given ventilation and heating

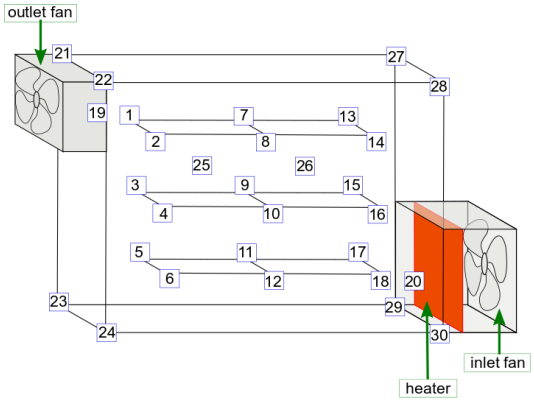

Fig. 1. Laboratory forced ventilation test chamber. The numbers represent the position of thermocouples.

combination (Tsitsimpelis and Taylor, 2015). The temperature within each zone is represented using TF models. Discrete–time models are selected below so that they can be directly used for digital control (e.g. Taylor et al., 2004b,a). However, the models identified are subsequently interpreted in continuous–time terms i.e. using appropriate dynamic heat balance differential equations.

2.3 Laboratory Experiments

The micro–climate within the 2 m × 1 m × 2 m forced ventilation chamber, illustrated in Fig. 1, is monitored using an array of 30 thermocouples, with airflow sensors at the inlet and outlet. Note that 18 thermocouples are laid out evenly in a grid arrangement, with 12 more placed in the corners and inlet–outlet openings. Actuators include two axial fans and a 500 W heating element, used to generate various micro–climatic conditions. The heating element is housed within a 0.68 m × 0.68 m × 0.54 m box at the inlet. The other important metric is the diameter of the outlet and the opening between the main chamber and heater box, both of which are 13 cm in diameter. The operation of the chamber is controlled by National Instruments hardware/software.

3. CFD MODEL OPTIMISATION

For the CFD simulations reported below, the inputs are the speed of the outlet fan and the power dissipated by the heating elements. For each of these, the present article uses the convention of 0–100% of the maximum input. For the experimental chamber, this is equivalent to a DC voltage from the control computer in the range of 0–5 V.

3.1 Mesh Optimisation

The chamber geometry is first represented using Autodesk Inventor and imported into ANSYS. The purpose of meshing is to discretise this geometry into small enough segments (i.e. small 3D shapes such as tetrahedrons), so that solving the transport equations for each segment provides a holistic view of the behaviour of the entire model domain. Fig. 2 shows an illustrative, relatively coarse mesh arrangement. Nonetheless, there is a significant concentration of elements around the heater, associated with the small diameter and curvature of the heating element.

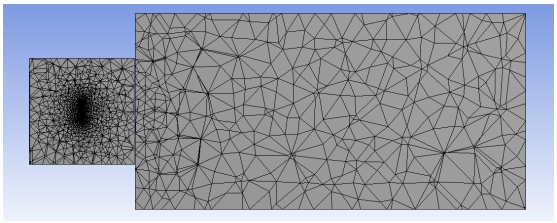

Fig. 2. Plan view of the chamber with an illustrative, relatively coarse mesh arrangement.

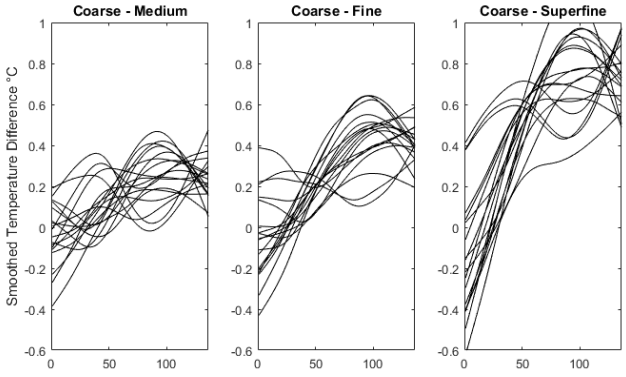

Fig. 3. Smoothed difference in temperature between the coarse mesh model and three other cases, plotted against sample number ($\Delta t = 2$ s).

Usually the simulation results will become more accurate as the mesh element size decreases, with an associated computational cost. Hence, a series of preliminary sensitivity simulations are undertaken based on inputs of 50% to the fan and heater. Temperature readings from 18 points corresponding to the thermocouple grid are recorded. Using the coarse mesh (Fig. 2) as the benchmark, Fig. 3 highlights the temperature differences between various other models. The coarse, medium, fine and superfine settings contain 200k, 250k, 350k and 1000k elements respectively. This is important because, while the differences in temperature between each subsequent mesh are up to approx. 0.2 degrees, these differences are not linearly related to the number of elements. Other common mesh statistics, such as skewness, are also considered (details omitted for brevity). The conclusion is that a mesh of approx. 1 million elements is satisfactory for the present purposes.

3.2 Boundary Conditions

Boundary conditions determine the methods and rate of exchange of mass and energy. For the chamber, air can only enter or leave via the inlet and outlet. By contrast, energy may be lost as heat through the walls and enters through the heating elements. The inlet is treated as an inlet–vent in Fluent, with zero gauge pressure difference over the boundary, hence allowing for recirculation in the heater box; and the outlet is modelled as a velocity inlet with negative velocity. The fluid is specified as air transporting water of mass fraction 0.005. The Perspex is 5 mm thick and has a thermal conductivity of 0.189 W m^{-2} K^{-1}. In practice, however, the dominant resistance to heat transfer is likely to be the wall to outside fluid interface since, for the chamber, this process is driven only by natural convection. The outside temperature is provided for each experiment, no–slip wall conditions are specified and, after consideration of Fourier's law and some practical experimentation, the estimated composite heat transfer coefficient $U = 4.9$ W m^{-2} K^{-1}.

Although the heater elements can, in principle, be modelled as a set of nickel–chrome alloy helices, the high complexity and associated long computation time is unnecessary given the other unknown element properties e.g. material composition, oxidation level, exact dimensions. Hence, the heater is modelled as a straightforward heat flux (W m^{-2}) based on three cylinders of radius 5 mm.

3.3 Solver

The coupled solver is selected i.e. pressure and velocity are solved concurrently. However, to reduce computational costs, turbulence is considered using transport equations that split the average and fluctuating parts of the Navier–Stokes equations. Since building environment models are relatively straightforward e.g. there are no supersonic flows nor aerofoils requiring sophisticated turbulence modelling, the shear stress transport model is selected.

3.4 Model Evaluation

With regard to airflow, one velocity transducer is permanently positioned at the outlet, since it provides the necessary velocity boundary condition; however, a second transducer is used to collect additional experimental data, in order to better understand the model performance. Fig. 4, for example, depicts the CFD modelled flow at relatively low (top figure) and medium (lower figure) velocities. In the former case, the air tends to move directly from the inlet to the outlet. By contrast, as the velocity increases, the incoming air predominantly moves horizontally before contacting the front chamber wall, followed by significant re-circulation around the chamber. These results are consistent with earlier smoke experiments and with *ad hoc* velocity measurements using the transducer.

However, for high velocities, the modelled airflow only consistently predicts experimental data near the inlet and outlet, with some significant modelling errors for the air velocity within the thermocouple grid. This may be connected to poor convergence of the velocity equations and needs further research. Nonetheless, in regard to the representation of *temperature*, the CFD model provides suitable initial estimates for the present purpose. To extract these temperature readings, an array of points are specified in the CFD post–processing module i.e. at equivalent positions to the thermocouples in the laboratory chamber. Since these locations are not necessarily on a node, the required temperatures are interpolated.

The absolute values of the temperature in the chamber are correctly predicted to within 1–2 degrees. However, the main weakness of the CFD model is that it often predicts less temperature variation between thermocouples than is observed in practice. To illustrate, Fig. 5 compares CFD and experimental data for one experiment, in which the heater input is changed between two levels. In addition, the CFD output can sometimes respond faster to changes in the input, again as illustrated in Fig. 5. This is because the CFD model predicts a greater air circulation towards

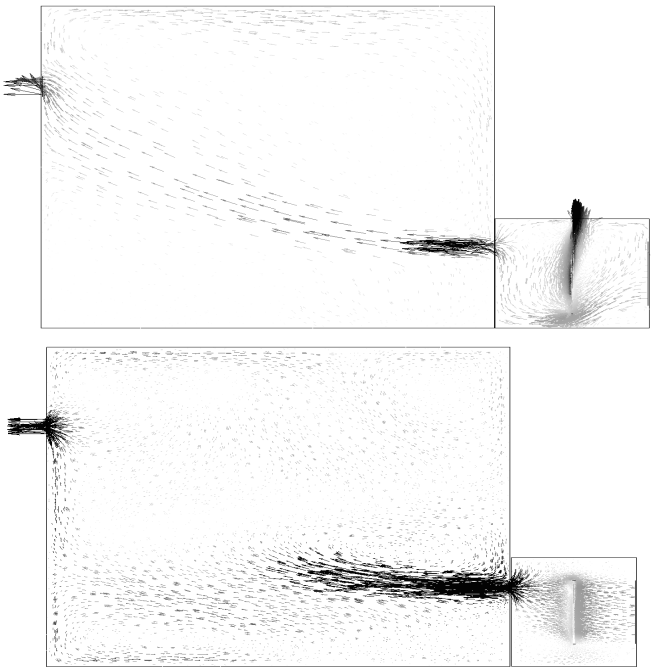

Fig. 4. Flow pattern generated by CFD model at the middle plane, with arrow length and tone both indicating velocity, from white at 0 m/s to black at 1 m/s. The heater box is shown bottom right and the extractor fan top left. Upper plot: fan input 30% and heater input 25%. Lower: fan 50% and heater 50%.

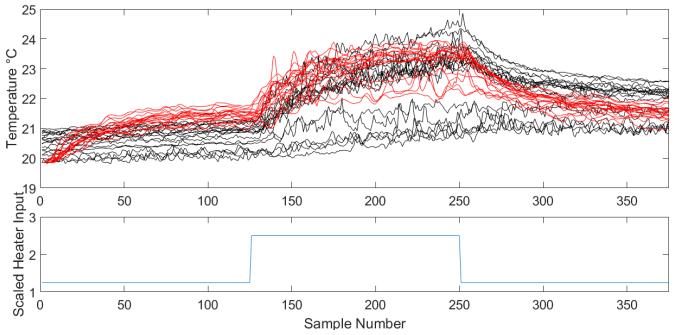

Fig. 5. CFD simulation (red) and experimental (black) temperature response at each thermocouple (upper plot) to step changes in the heater input (lower), plotted against sample number ($\Delta t = 4$ s), with the fan input 30% throughout.

the edges of the chamber than occurs in practice. This is likely to be related to the mesh structure and turbulence model. In addition, simulations show that the incoming air humidity can be an important factor in obtaining improved accuracy, and further analysis of the radiation properties of the chamber is also required. Finally, it possible that, over time, the chamber heats the surrounding laboratory air, something that is not presently modelled. All these issues are being investigated by the authors.

4. DBM MODEL

The SRIV algorithm, combined with R_T^2 and YIC identification criteria (e.g. Young, 2011; Taylor et al., 2013, Chapter 8), suggest that the following TF model adequately describes linear temperature dynamics in the chamber. This result applies for both experimental and CFD generated data. Furthermore, such models are utilised for each thermocouple (as illustrated below) or for the average temperature of well–mixed zones that have been statistically identified from data (Tsitsimpelis and Taylor, 2015). Here, the temperature of a thermocouple j ($j = 1, \ldots, 30$) is:

$$t_j(k) = \frac{b_0 + b_1 z^{-1}}{1 + a_1 z^{-1} + a_2 z^{-2}} u(k - \tau) \qquad (1)$$

where $t_j(k) = T_j(k) - \tilde{t}_j$ and $u(k) = U(k) - \tilde{u}$ are the sampled temperature and heater perturbations from the operating levels (i.e. $\tilde{t}_j$ and $\tilde{u}$), and $T_j(k)$ and $U(k)$ are the temperature (K) and heater input (%) respectively; τ is the time–delay in samples; $\{a_1, a_2, b_0, b_1\}$ are parameters; and z^{-1} is the backward shift operator, i.e. $y(k)z^{-1} = y(k-1)$. In fact, for the experimental scenarios considered here, the model (1) with $b_1 = a_2 = 0$ is most typically identified, and this result is consistent with the mechanistic interpretation below. Fig. 6 shows the response of this first order model for three, illustrative thermocouples, in this case for the CFD simulation output but similar model structures are obtained for experimental data.

The model (1) assumes time–invariant ventilation rate for a given experiment. Furthermore, as usual for a linear TF, it is based on relatively small perturbations of the temperature about an operating point and does not address system nonlinearities associated with particularly high or low heater settings. For consideration of multiple inputs and the framing of the TF model within a novel state–dependent parameter, Hammerstein system, see Tsitsimpelis and Taylor (2014). By contrast, the focus of the present article is to develop a straightforward mechanistic interpretation of (1). In this regard, on an assumption of a well mixed–zone, a classical heat balance differential equation takes the form (see e.g. Janssens et al., 2004),

$$\frac{dT_j(t)\mathrm{vol}_j \rho c_p}{dt} = V_c T_i(t - \tau_i)\rho c_p + Q_c(t - \tau_c) - (V_c T_j(t)\rho c_p + k_j S_j[T_j(t) - T_o(t)]) \qquad (2)$$

where $T_j(t)$ is the temperature of the air in a well–mixed zone (K), vol_j is the volume of the zone (m^3), ρ is the air density ($\mathrm{kg\ m^{-3}}$), c_p is the air heat capacity ($\mathrm{J\ kg^{-1}\ K^{-1}}$), V_c is the fraction of the total ventilation rate entering the zone, $T_i(t)$ is the temperature of the incoming air (from the heater box in this case), $Q_c(t)$ represents any directly added heat e.g. from an internal heater or room occupants ($\mathrm{j\ s^{-1}}$), k_j is the heat transfer coefficient ($\mathrm{J\ s^{-1}\ m^2\ k^{-1}}$), S_j is the contact area with the boundary (m^2) and $T_o(t)$ is the outside (here laboratory) temperature. Finally, τ_i and τ_c are time–delays (s) associated with the incoming air and internal heat source respectively.

Defining $t_j(t) = T_j(t) - \tilde{t}_j$ (cf. discrete–time equivalent, below equation (1)) and $t_i(t) = T_i(t) - \tilde{t}_i$, and assuming for this experiment that $Q_c = 0$ and T_o is time–invariant, then equation (2) simplifies to,

$$\frac{dt_j(t)}{dt} = -\alpha_j t_j(t) + \beta t_i(t - \tau_i) \qquad (3)$$

where $\alpha_j = \beta + k_j S_j / \mathrm{vol}_j \rho c_p$ and $\beta = V_c / \mathrm{vol}_j$. Note that it is straightforward to obtain a two–input, single

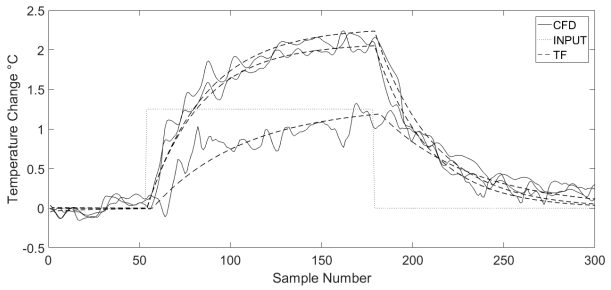

Fig. 6. TF model (dashed traces) and CFD simulation output (solid) temperature responses for thermocouples 1, 11 and 14 (see Fig. 1), with $\Delta t = 4$ s.

output model in which the laboratory temperature $T_o(t)$ represents the second input. The latter is omitted for brevity i.e. in the present analysis, the relatively small changes in $T_o(t)$ are ignored. However, an important novelty here, in comparison to the analysis of Janssens et al. (2004) and related references cited above, is the use of a similar heat balance equation for $T_i(t)$,

$$\frac{dT_i(t)\mathrm{vol}_i\rho c_p}{dt} = V_c T_o(t-\tau_o)\rho c_p + \gamma u(t-\tau_u) - (V_c T_i(t)\rho c_p + k_i S_i[T_i(t) - T_o(t)]) \quad (4)$$

In this case, vol_i is the volume of the heater box and it is assumed that the direct heat term is proportional the heater input $u(t)$; in future work, the model can be extended by using nonlinear heater relationships (Tsitsimpelis and Taylor, 2014). Assuming time–invariant T_o,

$$\frac{dt_i(t)}{dt} = -\alpha_i t_i(t) + \gamma u(t-\tau_u) \quad (5)$$

The significance of the second heat balance equation is that $u(t)$ directly represents a signal that will be used as the actuator in future control system design studies.

Substituting equation (5) into (3) yields a second order differential equation that, by means of an appropriate discrete–time approximation, yields the identified TF model (1), in which the composite sampled time–delay τ is based on the sum of τ_i and τ_u. Furthermore, since the time constant of the well mixed zone in the chamber $(1/\alpha_j)$ is much larger than that of the heater box $(1/\alpha_i)$, a further approximation is the first order TF model alluded to above i.e. based on equation (1) with $b_1 = a_2 = 0$. In other words, the heat balance model supports the results of the TF model system identification and hence, in general terms, also provides a link between the data–based and physical modelling approaches.

5. DISCUSSION & CONCLUSIONS

This article has considered both CFD and DBM models, as initially applied to a forced ventilation chamber but with the aim, in future work, to extend these concepts to the Lancaster University campus heating system, in addition to other bespoke problems such as agricultural grow–cells (Tsitsimpelis et al., 2016). The TF models associated with the DBM approach form an ideal basis for model reduction, emulation and control system design, all of which are important in the context of energy efficiency and thermal comfort in buildings. Such models can be identified from either measured or CFD generated data.

Lancaster University's Building Management System, or BMS, facilitates extensive data collection on the building state parameters and control inputs. Nonetheless, CFD modelling still provides two key advantages. In the first instance, a more detailed description of the room or zone in question is provided by the CFD model than is the case for measured data. The physical placement of sensors in buildings, often on ceilings, combined with the limited numbers of these sensors, can result in a data set that is ill–suited to monitoring the thermal conditions experienced by the building occupants (which is one of the primary optimisation objectives alluded to above). However, when combined with known dimensions of the room and other parameters that have direct physical meaning, such measured data *are* sufficient to create and optimise a CFD model. This allows the modeller to generate a representation of the conditions being experienced by the room occupants under a range of scenarios, rather than being constrained to specific sensor locations.

Secondly, CFD models facilitate investigations into the thermal properties of various zones of interest, without requiring additional data collection. For example, the CFD model can generate simulation data to represent exceptional operating conditions that are not necessarily covered by existing BMS data e.g. central boiler failure or extreme weather conditions. Furthermore, the estimation of suitable low order models for control system design, using planned open–loop experiments based on optimally designed input signals for system identification purposes, can be conducted using the CFD model, something that is usually impracticable in occupied buildings.

With regard to the specific ANSYS model created and optimised for a laboratory test chamber, as considered in this article, the model is presently capable of simulating the temperature response of the chamber for different heater and fan settings, yielding responses that are broadly equivalent to experimental data. Whilst some important aspects of the physical chamber have been incorporated into the CFD model, such as convective heat transfer through the walls, other factors have not yet been thoroughly investigated. These include the humidity and radiation elements of the model that are the subject of current research by the authors. Lessons learnt in regard to meshing, boundary conditions and data extraction, are now being applied to the wider aims of the project. Temperature and ventilation time–series data for zones in a modern campus building, namely the free–standing Charles Carter Building, are being extracted from the BMS logs. In future work, the CFD model developed above will be adapted to provide detailed information of the zones in this building.

The Charles Carter Building lies in the south part of the university's main campus, with a footprint of 33 m by 36 m and four floors. Internally the building is laid out around a central atrium that is open from the floor to the roof. Surrounding this area are lecture theatres, offices, meeting rooms and break-out spaces. Most typically in the literature, thermal zones are selected using building schematics. For example, Mayer et al. (2017) quarter a floor into four zones. By contrast, recent research by Tsitsimpelis and

Taylor (2015) show that zone selection can instead be temperature data–driven, as part of an extended DBM modelling framework. In the present project, a suite of TF models will be identified for all the zones, yielding a matrix of models to represent the entire building. At this stage, the modelling framework will be incorporated into a predictive building level controller, and linked to the supply network and other buildings, with the aim of improving the energy efficiency and robustness of the campus wide system.

While demand–side controllers already exist (Kim, 2013), one novelty in the planned algorithm is the need to address multiple buildings on this linked network, each modelled using the DBM methods described above. Finally, the campus energy centre has multiple ways of producing hot water (gas boilers as well as combined heat and power) and incorporating this added element of production choice will add further challenge to the optimisation problem.

REFERENCES

Agbi, C., Song, Z., and Krogh, B. (2012). Parameter identifiability for multi–zone building models. In *51st IEEE Conference on Decision and Control*. Maui, Hawaii.

Desta, T., Janssens, K., Van Brecht, A., Meyers, J., Baelmans, M., and Berckmans, D. (2004a). CFD for model–based controller development. *Building and Environment*, 39, 621–633.

Desta, T., Van Brecht, A., Meyers, J., Baelmans, M., and Berckmans, D. (2004b). Combining CFD and data–based mechanistic (DBM) modelling approaches. *Energy and Buildings*, 36, 535–542.

Foucquier, A., Robert, S., Suard, F., Stéphan, L., and Jay, A. (2013). State of the art in building modelling and energy performances prediction: A review. *Renewable and Sustainable Energy Reviews*, 23, 272–288.

Goyal, S., Ingley, H.A., and Barooah, P. (2013). Occupancy–based zone–climate control for energy–efficient buildings: Complexity vs. performance. *Applied Energy*, 106, 209–221.

Hong, S.W., Exadaktylos, V., Lee, I.B., Amon, T., Youssef, A., Norton, T., and Berckmans, D. (2017). Validation of an open source CFD code to simulate natural ventilation for agricultural buildings. *Computers and Electronics in Agriculture*, 38, 80–91.

Ioannou, E. (2016). *Modelling to improve the energy efficiency of space heating on campus*. Master's thesis, Engineering Department, Lancaster University.

Janssens, K., Van Brecht, A., Zerihun Desta, T., Boonen, C., and Berckmans, D. (2004). Modeling the internal dynamics of energy and mass transfer in an imperfectly mixed ventilated airspace. *Indoor Air*, 14, 146–153.

Kim, S.H. (2013). Building demand–side control using thermal energy storage under uncertainty: An adaptive multiple model–based predictive control (MMPC) approach. *Building and Environment*, 67, 111–128.

Kossak, B. and Stadler, M. (2015). Adaptive thermal zone modeling including the storage mass of the building zone. *Energy and Buildings*, 109, 407–417.

Lazos, D., Sproul, A.B., and Kay, M. (2014). Optimisation of energy management in commercial buildings with weather forecasting inputs: A review. *Renewable and Sustainable Energy Reviews*, 39, 587–603.

Mayer, B., Killian, M., and Kozek, M. (2017). Hierarchical model predictive control for sustainable building automation. *Sustainability*, 9, 1–20.

Mirinejad, H., Welch, K.C., and Lucas, S. (2012). A review of intelligent control techniques in HVAC systems. In *IEEE Energytech*. Cleveland, USA.

Paulus, M.T., Claridge, D.E., and Culp, C. (2015). Algorithm for automating the selection of a temperature dependent change point model. *Energy and Buildings*, 87, 95 – 104.

Price, L., Young, P.C., Berckmans, D., Janssens, K., and Taylor, C.J. (1999). Data–based mechanistic modelling (DBM) and control of mass and energy transfer in agricultural buildings. *Annual Reviews in Control*, 23, 71–83.

Ryozo, O. and Kazuhiko, K. (2009). Optimal design method for building energy systems using genetic algorithms. *Building and Environment*, 44, 1538–1544.

Steeman, H.J., Janssens, A., Carmeliet, J., and De Paepe, M. (2009). Modelling indoor air and hygrothermal wall interaction in building simulation: Comparison between CFD and a well–mixed zonal model. *Building and Environment*, 44, 572–583.

Taylor, C.J., Leigh, P., Price, L., Young, P.C., Berckmans, D., Janssens, K., Vranken, E., and Gevers, R. (2004a). Proportional–integral–plus (PIP) control of ventilation rate in agricultural buildings. *Control Engineering Practice*, 12, 225–233.

Taylor, C.J., Leigh, P.A., Chotai, A., Young, P.C., Vranken, E., and Berckmans, D. (2004b). Cost effective combined axial fan and throttling valve control of ventilation rate. *IEE Proceedings: Control Theory and Applications*, 151, 577–584.

Taylor, C.J., Pedregal, D.J., Young, P.C., and Tych, W. (2007). Environmental time series analysis and forecasting with the Captain Toolbox. *Environmental Modelling and Software*, 22, 797–814.

Taylor, C.J., Young, P.C., and Chotai, A. (2013). *True Digital Control: Statistical Modelling and Non–Minimal State Space Design*. John Wiley and Sons.

Taylor, C.J., Young, P.C., Tych, W., and Wilson, E.D. (2018). New developments in the CAPTAIN Toolbox for Matlab. In *18th IFAC Symposium on System Identification, Stockholm*.

Tsitsimpelis, I. and Taylor, C.J. (2014). A 2–dimensional Hammerstein model for heating and ventilation control of conceptual thermal zones. In *10th UKACC International Control Conference*. Loughborough, UK.

Tsitsimpelis, I. and Taylor, C.J. (2015). Partitioning of indoor airspace for multi–zone thermal modelling using hierarchical cluster analysis. In *14th European Control Conference*. Linz, Austria.

Tsitsimpelis, I., Wolfenden, I., and Taylor, C.J. (2016). Development of a grow–cell test facility for research into sustainable controlled–environment agriculture. *Biosystems Engineering*, 150, 40–53.

Yang, R. and Wang, L. (2013). Multi–zone building energy management using intelligent control and optimization. *Sustainable Cities and Society*, 6, 16–21.

Young, P.C. (2011). *Recursive Estimation and Time Series Analysis: An Introduction for the Student and Practitioner*. Springer.